INVESTIGATION OF THE STRUCTURAL DISORDER IN ICE Ih USING NEUTRON DIFFRACTION AND REVERSE MONTE CARLO MODELLING

L. Temleitner and L. Pusztai

Research Institute for Solid State Physics and Optics, Hungarian Academy of Sciences, Budapest, P.O. Box 49., H-1525, Hungary

1 INTRODUCTION

Although the crystallographic structure of the most common form of ice, phase Ih, has been known for many decades[1], its proton-disordered local structure is still being discussed[2,3]. As a demonstration of this fact, we mention that the geometry of water molecules in ice Ih has only recently been determined accurately, with the help of rather sophisticated quantum mechanical calculations[3].

Apart from Bragg-scattering (which is the main concern of classical crystallography), the experimentally measurable neutron diffraction pattern of ice Ih displays a rather characteristic diffuse signal, as was shown, e.g., in Ref.[4]. In most crystallographic studies, this part of the powder pattern is considered as 'background' and is subtracted from the measured data, since it has no effect on the translational symmetry of the crystal. Diffuse scattering, on the other hand, carries information on the local (dis)order which for ice Ih, that was described as a 'proton glass' (as opposed to a 'proton crystal')[3], may apparently be an important and integral part of the structure.

Total neutron scattering data (including diffuse scattering) from ice Ih have been made use by Floriano et al.[5], who derived parameters concerning only the molecular structure via Fourier transforming the measured structure factor. Later, the approach of Nield et al.[6,7,8] has included Reverse Monte Carlo (RMC) structural modelling[9] of single crystal neutron diffraction data. Their method, which did not consider Bragg-scattering during the calculations, applied a special computer code dubbed as 'RMCX'. Although RMCX has not been further developed over the past decade, the work of Nield and co-workers showed that studying the diffuse scattering contribution may lead to a deeper understanding of the behaviour of ice Ih.

In this contribution, we report a neutron powder diffraction study of ice Ih at 120 and 200 K. The data, including Bragg and diffuse scattering, were interpreted by the RMCPOW (Reverse Monte Carlo for POWder diffraction data) method[10], using large (containing, e.g., 8x8x8 unit cells, that is, more than 2000 molecules) three dimensional models. RMCPOW is based on the standard RMC algorithm[9] and aims at matching the full powder diffraction signal. Description of the diffuse scattering part is done by moving atoms around while maintaining the long range ordering of the crystal. The resulting

particle configurations are analysed in terms of partial radial distribution functions and cosine distribution of bond angles – similarly to a liquid/amorphous structure. RMCPOW is faster and more general than RMCX; in addition, powder diffraction data are a lot easier to take and handle than single crystal data. For these reasons it is foreseen that the combination described in the present contribution (powder diffraction + RMCPOW modelling) may be used more widely in the future.

2 NEUTRON DIFFRACTION EXPERIMENT

Neutron powder diffraction experiments on fine D_2O ice powder have been carried out using the NPD two-axis diffractometer installed at Studsvik NFL (Sweden; the facility was, regrettably, phased out in 2005). A Ge (2 2 0) monochromator provided a neutron beam with a wavelength of 1.47 Å, so that a scattering vector (Q) range of 0.3 – 8 $Å^{-1}$ could be covered. The sample was filled in a 10 mm diameter vanadium container; the container then was placed within a standard CCR. In order to minimise the effects of preferred orientation of ice crystallites, the whole setup was rotated during the experiment. Measurements on the empty sample holder, as well as of a bulk vanadium rod (as incoherent scatterer) have also been performed, at the temperatures of the ice measurements (120 and 200K). Raw data have been treated the same way as liquids/amorphous diffraction results, i.e., corrections for instrumental background, detector efficiency, absorption and multiple scattering, as well as absolute normalisation (with respect to an incoherent scatterer) have been carried out.

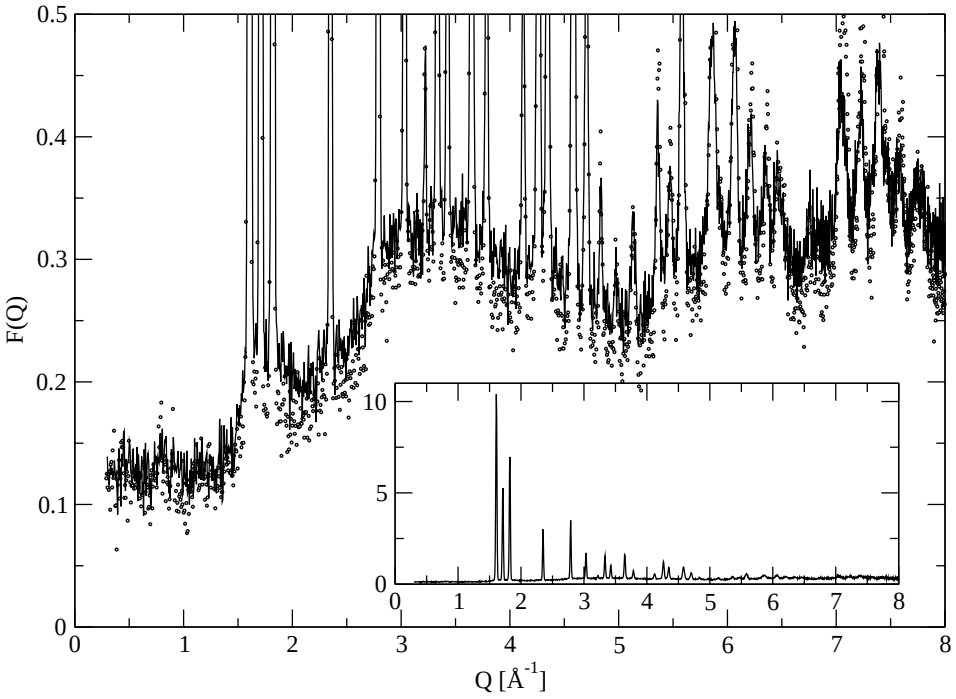

Figure 1 *Large panel: measured powder diffraction pattern of (D_2O) ice Ih at 120 K (symbols) and 200 K (solid line); the focus is on the diffuse scattering part. Insert: powder diffraction pattern of ice Ih at 200 K.*

Figure 1 shows the corrected and normalised total scattering functions, *F(Q)*, of ice Ih at two temperatures, 120 and 200 K. The enhanced level of diffuse scattering at 200 K may be observed.

3 STRUCTURAL MODELLING – RESULTS

The RMCPOW calculations were started from initial configurations that obeyed the 'ice-rules'[11] and possessed no net dipole moments. For generating the starting coordinates, a slightly modified version of the algorithm of Barkema et al.[12] has been applied. By using supercells of 2^3, 4^3, 8^3 and 11x12x7 unit cells of hexagonal ice I it could be established that results to be presented here show no dependence on the system size (apart from statistics). We found the 8^3 unit cell system convenient (large enough but the computational costs were not too high) and therefore, properties of such systems will be discussed below.

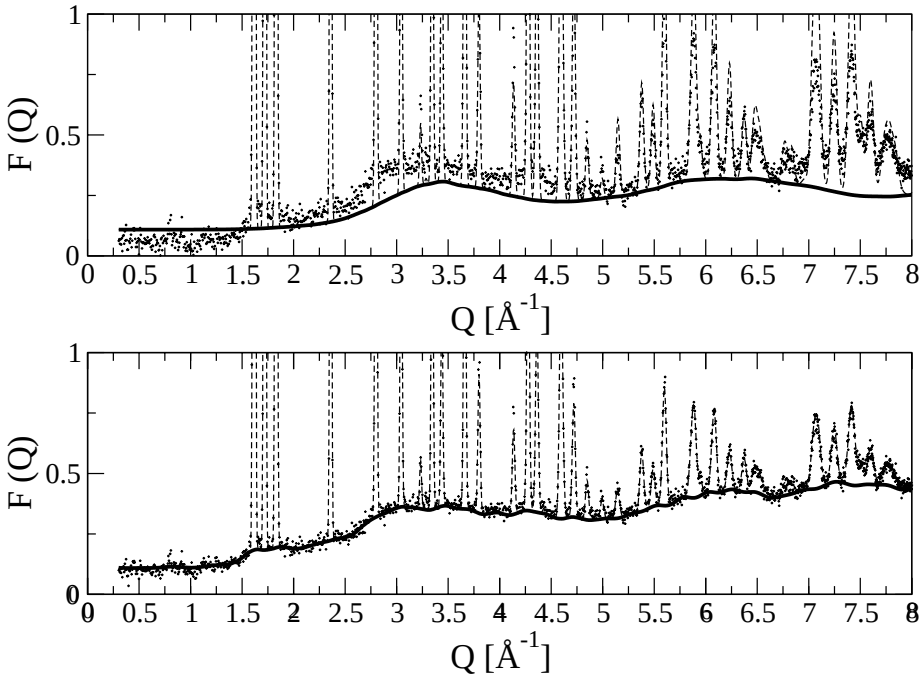

Figure 2 *Upper panel: measured powder diffraction pattern of (D_2O) ice Ih at 120 K (symbols) as compared to that of the initial configuration (dashed line); the diffuse part is also shown (thick solid line). Lower panel: RMCPOW fit to the measured signal (dashed line); the diffuse part is also given (thick solid line).*

Figures 2 and 3 compare measured and simulated total scattering functions (tsf) for ice Ih at 120 and 200 K, respectively. The upper panels of Figures 2 and 3 compare tsf's for the initial stages of the RMCPOW modelling. It is obvious that Bragg scattering, as far as peak positions are concerned, is well described by the starting configurations, although intensities may not always match the measured values. Note, however, that the shape and intensity of the diffuse part had to change enormously between the initial and final states of the calculations.

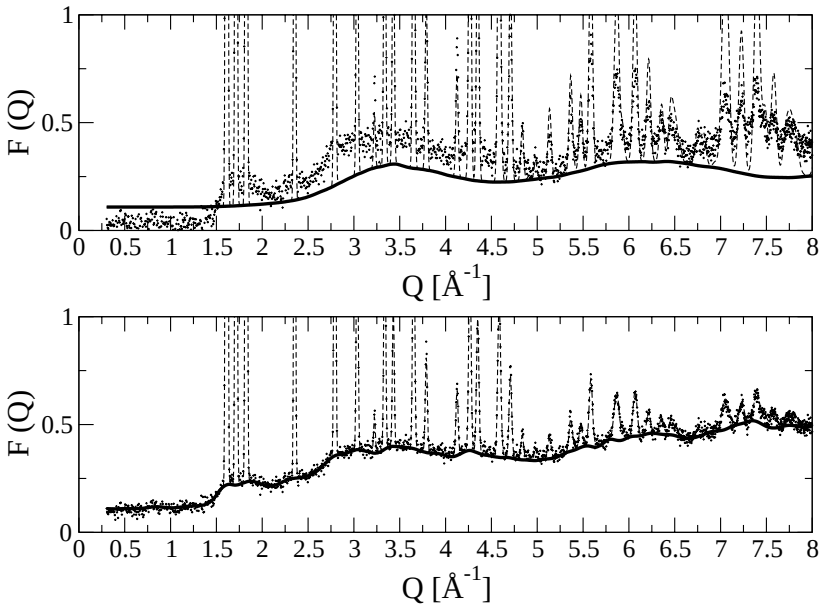

Figure 3 *Upper panel: measured powder diffraction pattern of (D_2O) ice Ih at 200 K (symbols) as compared to that of the initial configuration (dashed line); the diffuse part is also shown (thick solid line). Lower panel: RMCPOW fit to the measured signal (dashed line); the diffuse part is also given (thick solid line).*

We must declare here that the entire study should be considered as a 'pilot project', with numerous details still to be clarified/refined. Still, the above finding seems to indicate that an important aspect of the structure of ice Ih, represented by the measured diffuse scattering, could not be captured sufficiently well by existing models of the crystalline structure.

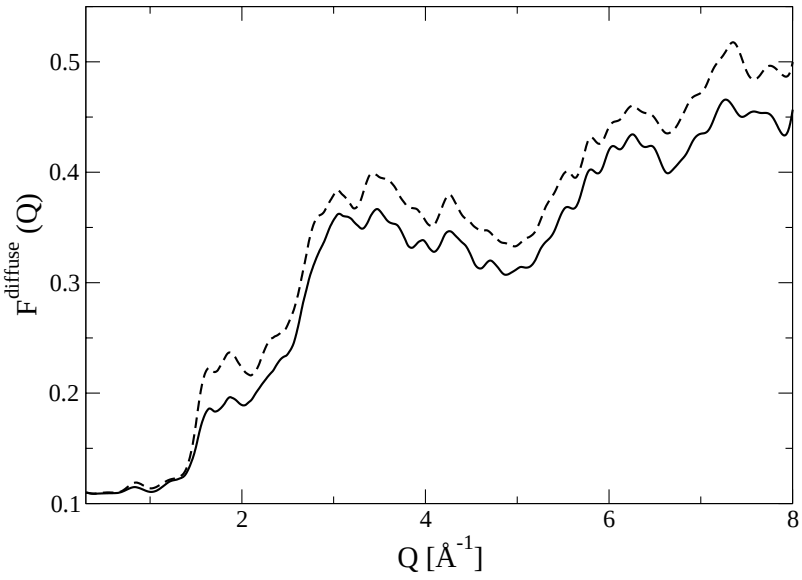

Figure 4 *Diffuse scattering from (D_2O) ice Ih at 120 K (solid line) and 200 K (dashed line), as calculated from RMCPOW.*

In Figure 4, diffuse scattering contributions are compared for the 120 and 200 K states. As it could be expected, the curves show similar features, except around the first maximum, just below 2 $Å^{-1}$. This – small, but apparent – difference may indicate that the structure might vary as the temperature increases beyond the level that would be expected on the basis of the stronger thermal vibrations. For being able to - at least – speculate about the origin of this variation we must switch from reciprocal to real space.

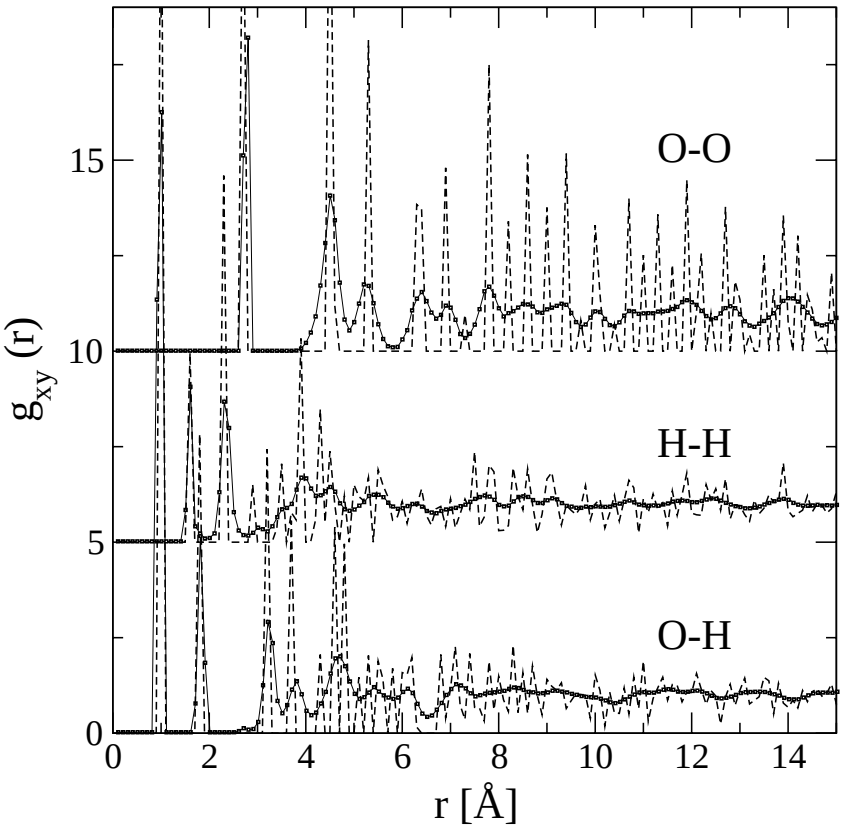

Figure 5 *Comparison of the partial pair correlation functions for the initial (dashed lines) and final (solid lines) stages at 120 K. In both cases, systems of 8^3 unit cells were applied.*

Initial and final O-O, O-H and H-H partial radial distribution functions (prdf) at 120 K are compared in Figure 5. The changes between the two stages are obvious, particularly as far as the O-O prdf is concerned: every single narrow initial peak has broadened (although still recognisable in the final stage). Most of these changes may be attributed to the effects of thermal vibrations, which are absent in the starting particle arrangement. The situation is less clear in this respect for the H-H and O-H prdf's which were affected by the 'proton-glass' nature of (even ideal) ice Ih. In any case, it has to be acknowledged that the differences between initial and final prdf's are the real space manifestations of the differences between initial and final diffuse scattering, shown in Figure 2 for the 120 K system. (It may be instructive to notice that the O-O part of Figure 5 can be considered as a demonstration of the difference between ideal and real crystalline behaviour.)

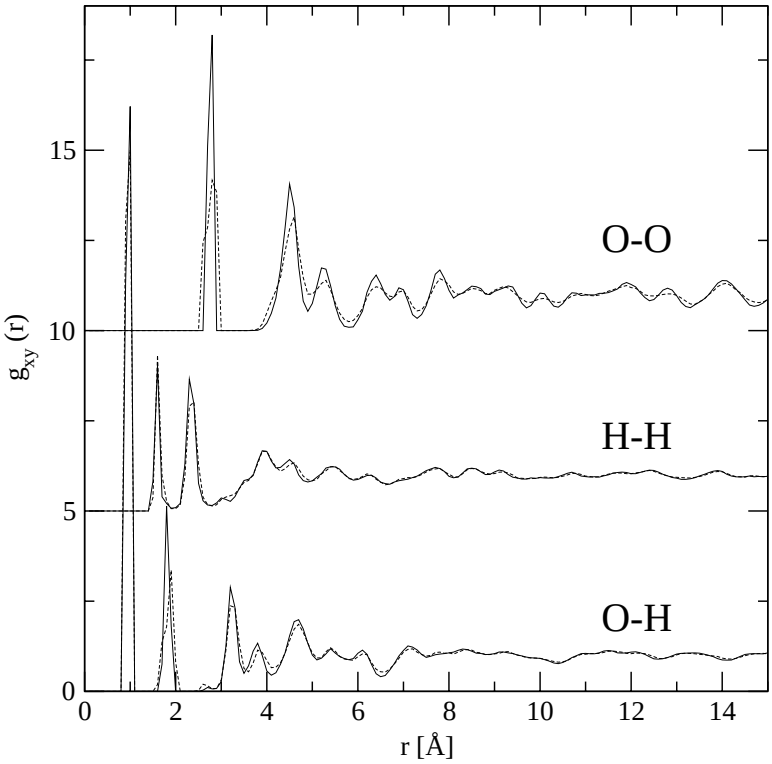

Figure 6 *Comparison of the partial pair correlation functions for the 120 K (solid lines) and 200 K (dashed lines) states. In both cases, systems of 8^3 unit cells were applied.*

Figure 6 provides the comparison of the three prdf's obtained for the 120 and 200 K states. The two sets of curves are rather similar, as it can be expected for the material in the given temperature range (far from the melting point). The H-H prdf's are nearly identical; there are, however, small alterations in terms of the O-O and O-H prdf's. For the former, the fist and second maxima seem to be shifted slightly towards higher *r* values, whereas for the latter, it is the first and third intermolecular peaks (just below 2 and just below 4 $Å^{-1}$, respectively) that behave similarly. The exact value of the shift is hard to tell at this stage, because of the – for this purpose, too – coarse *r*-spacing that was applied while calculating prdf's. (The given value of 0.1 Å was required for achieving reasonable statistics.) It will be necessary to take a closer look at these small variations (e.g., by further increasing the size of the system and thus allowing for a better *r*-resolution); what can be stated already at this stage is that the changes are the *r*-space manifestations of the difference of the diffuse scattering signal found to be present between the investigated two states of ice Ih (see Figure 4). It can also be suggested that the differences are connected to the hydrogen bonding network of ice Ih: hydrogen bonds appear to be somewhat longer at 200 K.

From the particle configurations provided by RMCPOW modelling it is possible to calculate any characteristics of the structure, including ones that go beyond two-particle properties. One of the simplest possibilities is to consider angular distributions. In Figure 7, two of these distributions, connected directly to hydrogen bonding, are presented for the starting configuration and for the final stages at 120 and 200 K. The distribution of the cosines of O…O…O angles show a continuous (and symmetric) broadening as

temperature increases; the position of the maximum, however, remains at -1/3, which is the value for the tetrahedral angle. The distribution of the O-H…O angles also indicates distortion of the straight angle that characterises hydrogen bonds in the ideal ice Ih crystal. The difference between the tails at 120 and 200 K seems to be a direct consequence of the slightly different diffuse scattering contributions at the two temperatures (see Figure 4).

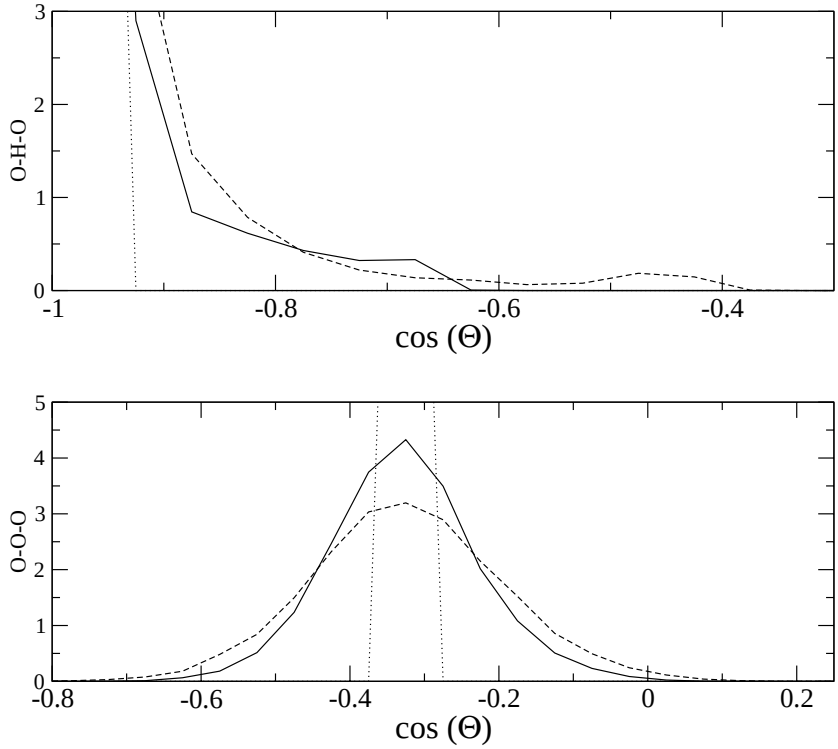

Figure 7 *Cosine distributions of O-H...O (upper panel) and O...O...O (lower panel) angles ("-" stands for intra-, whereas "…" stands for intermolecular connections). Dotted line: initial configuration; solid line: 120 K; dashed line: 200 K.*

4 SUMMARY AND OUTLOOK

It is shown that both the Bragg and the diffuse scattering parts of neutron powder diffraction data on ice Ih can be interpreted simultaneously by constructing large models of the structure that are consistent with the measured total scattering functions within errors. The RMCPOW algorithm[10] proved to be readily applicable for the purpose.

It is found that proton disorder on its own cannot be responsible for the measured level and shape of diffuse scattering. The present results, particularly the O-H and O-O partial radial distribution functions and the distribution of the O-H…O hydrogen bond angles suggest that small changes of the hydrogen bonded network are most probably responsible for the slightly different shape of the diffuse scattering signal at 120 and 200 K.

In this pilot study, ice Ih was considered in a 'safe' temperature range, between 120 and 200 K. For improving the reliability of the results presented here, an obvious extension would be an X-ray diffraction measurement (also of the 'total scattering type') and the subsequent RMCPOW modelling of both the neutron and X-ray data together. Using such a combination, approaching the melting point would be easier to achieve; investigations on

this ‘high temperature’ ice Ih are expected to provide valuable information on the behaviour hydrogen bonded network of water molecules during the process of melting. It is also worth mentioning that similar studies may be carried out on other phases of ice, too, provided that the appropriate total scattering type diffraction data are available.

Acknowledgment

LP is grateful to the staff of Studsvik NFL (Sweden) for their hospitality while staying with them and for their help with the numerous experiments on ice Ih powder. He is also grateful to Dr. V.M. Nield, for her help with the initial ice powder experiment on the SLAD diffractometer in Studsvik. Financial support for this work was provided by the OTKA (Hungarian Basic Research Fund), grant Nos. T048580 and T043542.

References

1 S.W. Peterson and H.A. Levy, *Acta Cryst.*, 1957, **10**, 1105.
2 S.W. Rick and A.D.J. Haymet, *J. Chem. Phys.*, 2003, **118**, 9291.
3 J.-L. Kuo, M.L. Klein and W.F. Kuhs, *J. Chem. Phys.*, 2005, **123**, 134505.
4 A.J. Leadbetter, R.C. Ward, J.W. Clark, P.A. Tucker, T. Matsuo and H. Suga, *J. Chem. Phys.*, 1985, **82**, 424.
5 M.A. Floriano, D.D. Klug, E. Whalley, E.C. Svensson, V.F. Sears and E.D. Hallman, *Nature*, 1987, **329**, 821.
6 V.M. Nield and R.W. Whitworth, *J. Phys.: Condens. Matter*, 1995, **7**, 8259.
7 M.N. Beverley and V.M. Nield, *J. Phys.: Condens. Matter*, 1997, **9**, 5145.
8 M.N. Beverley and V.M. Nield, *J. Phys. Chem. B*, 1997, **101**, 6188.
9 R.L. McGreevy and L. Pusztai, *Molec. Simul*., 1988, **1**, 359.
10 A. Mellergård and R.L. McGreevy, *Acta Cryst*., 1999, **A55**, 783.
11 J.D. Bernal and R.H Fowler, *J. Chem. Phys.*, 1933, **1**, 515.
12 G.T. Barkema and M.E.J. Newman, *Phys. Rev. E*, 1998, **57**, 1155.